energies

MDPI

Article

Research on Defect Detection for Overhead Transmission Lines Based on the ABG-YOLOv8n Model

Yang Yu, Hongfang Lv *, Wei Chen and Yi Wang

School of Electrical Engineering, Shanghai Dianji University, Shanghai 201306, China; 19901671369@163.com (Y.Y.); 18787152082@163.com (W.C.); 18061847267@163.com (Y.W.)
* Correspondence: lvhf@sdju.edu.cn

Abstract: In the field of smart grid monitoring, real-time defect detection for overhead transmission lines is crucial for ensuring the safety and stability of power systems. This paper proposes a defect detection model for overhead transmission lines based on an improved YOLOv8n model, named ABG-YOLOv8n. The model incorporates four key improvements: Lightweight convolutional neural networks and spatial–channel reconstructed convolutional modules are integrated into the backbone network and feature fusion network, respectively. A bidirectional feature pyramid network is employed to achieve multi-scale feature fusion, and the ASFF mechanism is used to enhance the sensitivity of YOLOv8n's detection head. Finally, comprehensive comparative experiments were conducted with multiple models to validate the effectiveness of the proposed method based on the obtained prediction curves and various performance metrics. The validation results indicate that the proposed ABG-YOLOv8n model achieves a 4.5% improvement in mean average precision compared to the original YOLOv8n model, with corresponding increases of 3.6% in accuracy and 2.0% in recall. Additionally, the ABG-YOLOv8n model demonstrates superior detection performance compared to other enhanced YOLO models.

Keywords: lightweighting; bidirectional paths; spatial and channel reconstruction; cross-scale feature fusion; ASFF mechanism

check for updates

Citation: Yu, Y.; Lv, H.; Chen, W.; Wang, Y. Research on Defect Detection for Overhead Transmission Lines Based on the ABG-YOLOv8n Model. *Energies* **2024**, *17*, 5974. https://doi.org/10.3390/en17235974

Academic Editor: Claus Leth Bak

Received: 13 October 2024
Revised: 15 November 2024
Accepted: 21 November 2024
Published: 27 November 2024

Copyright: © 2024 by the authors. Licensee MDPI, Basel, Switzerland. This article is an open access article distributed under the terms and conditions of the Creative Commons Attribution (CC BY) license (https://creativecommons.org/licenses/by/4.0/).

1. Introduction

Overhead transmission lines are a crucial component of the power system, and their stable operation is essential to ensuring the safe and reliable delivery of electricity [1]. However, being exposed to external environments, these lines are susceptible to various external factors that can lead to defects, thereby affecting the stability of the power supply [2,3]. As a result, regular inspection and maintenance of overhead transmission lines have become key tasks for power companies and relevant authorities [4,5].

Traditional methods for inspecting overhead transmission lines mainly rely on manual inspection, which is not only time-consuming and labor-intensive but may also pose certain safety risks [6]. Moreover, the efficiency and accuracy of manual inspection are limited by the experience and skill level of the inspectors, making it difficult to efficiently and comprehensively identify potential issues [7]. With advancements in science and technology, automated detection methods based on computer vision and deep learning have gradually become a research hotspot [8]. By utilizing image processing and feature recognition techniques, these methods can detect various defects and anomalies in overhead transmission lines in a relatively short period, significantly improving inspection efficiency and accuracy. These approaches are gradually becoming the mainstream method for load forecasting in power systems [9,10].

In summary, the defect detection scheme for overhead transmission lines incorporating deep learning methods has more excellent performance compared with the traditional method [6,11]. Thus, it is an inevitable research trend to incorporate improved detection

algorithms into traditional detection methods to enhance the efficiency and accuracy of defect detection [12,13].

Automated detection methods based on computer vision and deep learning have been widely used in various fields in recent years, such as autonomous driving, security monitoring and medical image analysis [14]. With the development of deep learning, more improvements and innovations have been introduced into the algorithms, making them continuously improve in accuracy and efficiency. An improved Faster RCNN algorithm was proposed in [15] for the problem of defect detection of connector solder joints inside electronic products, using clustering to generate anchor frames and combining with ResNet-101 for migration learning, but the average detection accuracy only reaches 88%, which is slightly insufficient. Aiming at the problem of face local attribute detection in complex environments, a method based on an improved SSD network structure which optimizes the network structure to enhance the face local attribute detection ability was proposed in [16], but the inference speed of the improved model is reduced, which affects the real-time scene effect. An improved feature pyramid network (SA-FPN) proposed in [17] for the problem of human detection in crowded scenarios significantly improves the performance of the detector but does not completely eliminate the false alarms.

Compared to the above algorithms, the YOLO family of models is known for its unique single-stage detection mechanism, which is able to significantly reduce inference times while maintaining high accuracy [18].

Ref. [19] proposed an improved deep learning algorithm for the problem of insufficient performance in small target detection, utilizing the high efficiency of YOLOv3 in target detection to enhance the intelligent detection of pinhole defects in transmission lines. Ref. [20] proposed an improved YOLOv5 method for the problem of anti-breakage detection in transmission lines by replacing the CSPdarknet53 module with MobilenetV3 to enhance the feasibility of the application in edge equipment and demonstrated a considerable detection performance. Ref. [21] proposed an improved DCP-YOLOv8 method for the problem of multi-type defect detection in transmission lines. The method enhances the extraction of defect features by deformable convolution, but the model is not lightweight enough to be deployed in edge computing devices.

In order to improve defect detection for overhead transmission lines, this paper proposes an overhead transmission line defect detection model based on the improved YOLOv8n model, named ABG-YOLOv8n. The application advantages of the model are as follows:

1. Huawei's mobile model GhostNetV2 is used to replace the feature extraction network of YOLOv8n, which can significantly reduce the network parameters and computation amount compared to other feature extraction networks while maintaining good feature expression capability.
2. A Bidirectional Feature Pyramid Network (BiFPN) is used in the feature fusion layer to replace the Path Aggregation Network (PANet) in YOLOv8n, which further improves the performance of the model in multi-scale target detection and makes the detection results more accurate.
3. Spatial and Channel Reconstruction Convolution (SCConv) is used to replace the standard convolutional layer in YOLOv8n, which enhances the feature expression capability by processing spatial and channel information simultaneously, improves the detection accuracy and robustness, and captures the spatial relationship and channel features of the object more effectively.

The combination of BiFPN + SCConv does not increase the complexity of the model and it significantly enhances the model's detection capability compared to other combinations.

4. The ASFF mechanism is introduced in the detection head part, which dynamically adjusts the weights of feature maps of different scales, thus better combining the feature information of various sizes in target detection and improving the model's sensitivity to targets of different sizes and the detection accuracy.

The above improvements can effectively enhance the detection capability of the model and are suitable for deployment in resource-constrained edge computing devices to improve transmission line detection efficiency.

This paper is divided into three parts: The first part is the introduction, which introduces the limitations of the traditional transmission line detection methods and introduces the detection algorithm proposed in this paper. The second part describes the model improvement method in detail, and the third part introduces the experimental process and the experimental results.

2. Methods

This paper proposes a defect detection method for overhead transmission lines based on an improved YOLOv8n model to maintain the stable operation of the power system. First, Huawei's mobile model GhostNetV2 is used to replace the original YOLOv8n feature extraction network, reducing the network parameters and computational load. The BiFPN is employed to replace YOLOv8n's PANet, improving the model's accuracy in multi-scale object detection. SCConv is introduced to replace some convolutional layers in YOLOv8n, capturing object spatial relationships and channel features more effectively. Finally, the ASFF mechanism is incorporated to enhance the model's sensitivity and accuracy in detecting objects of different sizes.

2.1. YOLOv8n Model Network Architecture

YOLOv8n is the eighth-generation model in the YOLO series, designed to provide faster inference speeds and lower computational requirements while maintaining high accuracy [21,22], making it suitable for deployment on resource-constrained devices such as edge and mobile devices. The architecture of YOLOv8n inherits the design principles of previous YOLO generations while introducing new improvements that make the network more efficient and accurate. The network structure is shown in Figure 1.

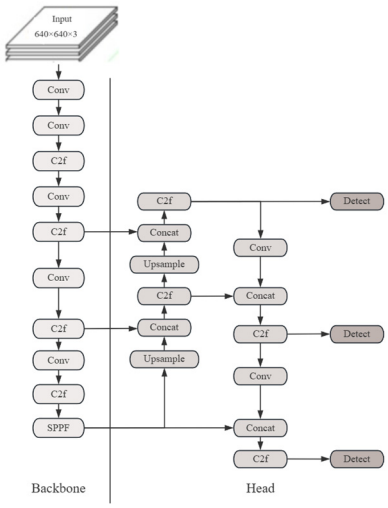


Figure 1. YOLOv8n model network structure diagram.

Overall, YOLOv8n is an efficient object detection model. Through its lightweight architecture design, it strikes a good balance between performance and computational resource demands.

2.2. Improved Training Model

This paper proposes an improved version of the YOLOv8n model, named ABG-YOLOv8n, which effectively enhances the detection accuracy of the model while making it more lightweight, reducing the consumption of computational resources. The network structure of the improved model is shown in Figure 2.

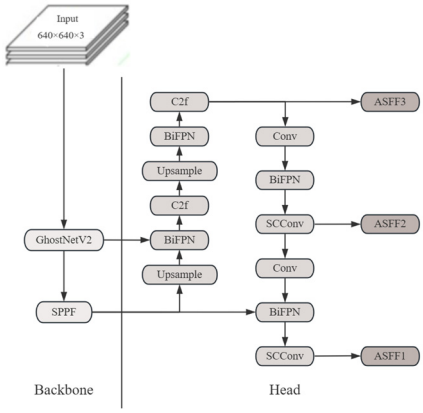


Figure 2. ABG-YOLOv8n model network structure diagram.

2.2.1. DFC Attention Mechanism

Huawei's mobile model GhostNetV2 serves as the new backbone network for the ABG-YOLOv8n model. Compared to the original backbone network, it is more lightweight, reducing the consumption of computational resources.

GhostNetV2 introduces a hardware-friendly attention mechanism called the DFC (Direction-Focused Convolution) attention mechanism. DFC is based on fully connected layers and is designed to execute quickly on general hardware while capturing long-range dependencies between pixels.

The information flow in the DFC attention mechanism is mainly divided into three parts: input feature decomposition, directional feature calibration, and attention map generation. The input feature map is decomposed into vertical and horizontal directional components. For each direction, a separate calibration process refines the feature representation, including scaling and stretching of the features to better capture information in the specific direction. Finally, the results from the vertical and horizontal directional calibrations are combined to generate a comprehensive attention map.

The feature representation of the input feature map in the vertical direction is expressed by Equation (1).

$$a'_{hw} = \sum_{h'=1}^{H} F^{H}_{h,h'w} \odot Z_{h'w} \tag{1}$$

where $F^{H}_{h,h'w}$ represents the feature calibration function in the vertical direction and $Z_{h'w}$ represents the corresponding output feature.

The feature representation of the input feature map in the horizontal direction is expressed by Equation (2).

$$a_{hw} = \sum_{h'=1}^{H} F^{W}_{w,hw'} \odot a'_{hw'} \tag{2}$$

where $F^{W}_{w,hw'}$ represents the feature calibration function in the horizontal direction and $a'_{hw'}$ represents the corresponding output feature.

2.2.2. Bidirectional Feature Pyramid Network

The ABG-YOLOv8n model introduces the BiFPN to replace the PANet in the feature fusion network of YOLOv8n, improving the model's performance in detecting targets at complex scales.

BiFPN is an efficient feature pyramid network that introduces bidirectional paths and cross-scale connections within the traditional feature pyramid structure. This allows features to be fused in both top-down and bottom-up directions, effectively combining features from different scales. The structure of the BiFPN network is shown in Figure 3.

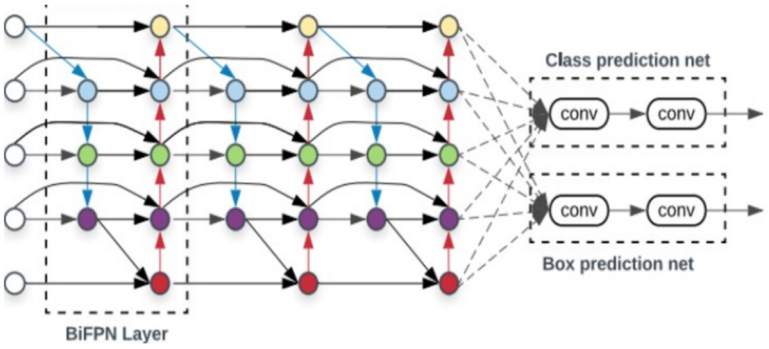


Figure 3. BiFPN network structure diagram.

In the top-down path, high-level features are progressively passed down to lower levels, where each level's features are fused with the current features through upsampling and a 1×1 convolution, enhancing the semantic information of high-level features while preserving the spatial accuracy of lower-level features. In the bottom-up path, the low-level, high-resolution features are processed and passed up to higher levels, with each level's features being fused with the higher level's features through downsampling, ensuring that the detailed low-level features can enhance the semantic information of the high-level features.

BiFPN specifically introduces a learnable weight coefficient to adjust the influence of different source features during the fusion process. The specific formula is shown in Equation (3).

$$O = \sum_{i}^{n} w_i \times I_i \tag{3}$$

where O is the output feature, I_i represents the input features obtained from different sources, and w_i is the corresponding learnable weight.

2.2.3. Spatial and Channel Reconstruction Convolution

The ABG-YOLOv8n model introduces Spatial and Channel Reconstruction Convolution (SCConv) to replace the standard convolution layers in the YOLOv8n model, improving the model's accuracy and robustness in detection.

SCConv can simultaneously process the shape, structure, color, and depth information of the image, making it not only suitable for image processing in complex scenes but also yielding significant improvements in small object detection and normal object detection. SCConv consists of two units: the Spatial Reconstruction Unit (SRU) and the Channel Reconstruction Unit (CRU). The Spatial Reconstruction Unit reduces spatial redundancy through separation and reconstruction methods, while the Channel Reconstruction Unit reduces channel redundancy using a split–transform–merge strategy. The structure diagram of SCConv is shown in Figure 4.

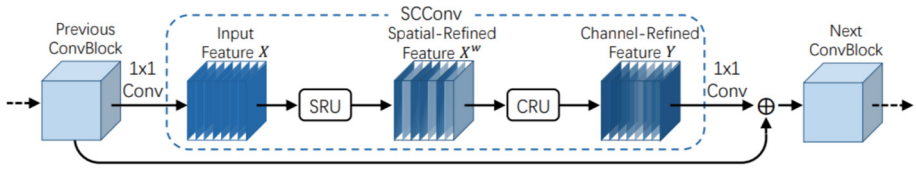


Figure 4. SCConv structure diagram.

The Spatial Reconstruction Unit (SRU) is responsible for reducing redundancy in the spatial dimensions of the feature map. It processes input features through four steps, as described below.

1. Group Normalization: The input features are normalized to reduce scale differences between different feature maps. The normalization formulas are as follows.

$$GN(x) = \gamma \frac{x - \mu}{\sqrt{\sigma^2 + \varepsilon}} + \beta \tag{4}$$

$$w_r = \{\omega_i\} = \frac{r_i}{\sum_{j=1}^{C} r_j}, i, j = 1, 2 \sim C \tag{5}$$

where C and γ are learnable parameters that measure the variance of the pixels within each batch and channel. These parameters are normalized between (0, 1) using Equation (4).

2. Weight Generation: Using normalization and the sigmoid activation function, weights are generated from the normalized feature map. The weight generation formula is as follows.

$$W = Gate(Sigmoid(Wr(GN(X)))) \tag{6}$$

3. Feature Separation: The input features are separated into multiple sub-feature sets based on the generated weights.
4. Feature Reconstruction: The separated features undergo transformation and recombination, producing spatially refined feature outputs.

The Channel Reconstruction Unit (CRU) is responsible for further refining the features by enhancing interactions between channels and improving information fusion. This is achieved through the following three steps:

1. Segmentation: The input feature map is divided into two parts, allowing different processing for each component in subsequent steps. The segmentation expressions are as follows:

$$x_{up} = Conv_{1\times1}(x^w, \alpha C) \tag{7}$$

$$x_{low} = Conv_{1\times1}(x^w, (1 - \alpha)C) \tag{8}$$

where αC and $(1 - \alpha)C$ represent the number of channels used.

2. Transformation: Using global convolution (GWC) and pointwise convolution (PWC), x_{up} and x_{low} are transformed. The transformation expression is as follows:

$$Y = PWC(GWC(X)) \tag{9}$$

3. Fusion: $Y1$ and $Y2$ are importance-weighted using Pooling and the SoftMax function, then combined through element-wise multiplication and addition to form the final channel-refined feature Y. The fusion expressions are as follows:

$$S = SoftMax(Pooling(Y)) \tag{10}$$

$$Y = S1 \otimes Y1 + S2 \otimes Y2 \tag{11}$$

where S represents the scaling factor and $\otimes$ denotes element-wise multiplication.

2.2.4. ASFF Mechanism

The Adaptive Spatial Feature Fusion (ASFF) mechanism is a feature fusion technique used in object detection networks. Its primary purpose is to enhance the fusion of information between features at different scales, thereby improving the accuracy and robustness of object detection. The working principle of ASFF is illustrated in Figure 5.

ASFF is mainly implemented through the following three steps for dynamic feature fusion.

1. Adaptive Scale Feature Extraction: For multiple feature layers in the object detection network, ASFF first processes each feature layer to ensure effective feature fusion.
2. Adaptive Weight Learning: Using the SoftMax function, the model learns the weights between different feature layers, dynamically adjusting their influence during the final feature fusion.

3. Feature Fusion and Prediction: After adjusting the weights, the feature layers are combined through weighted summation. The fused features are then used for subsequent object detection tasks.

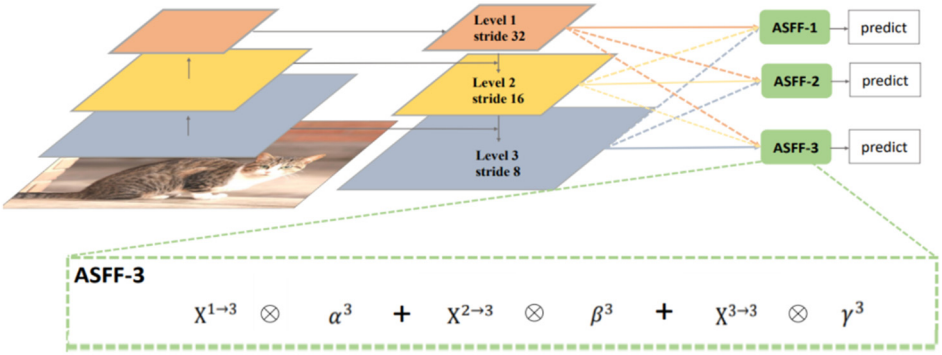


Figure 5. ASFF working principle diagram.

3. Experimental Results and Analysis

3.1. Data Processing and Model Prediction

The experimental hardware environment is shown in Table 1. The software environment includes Python 3.9, PyTorch 1.12.1, CUDA 11.6, and CUDNN v8.9.7.

Table 1. Experimental hardware environment.

Hardware	Model	Quantity
CPU	Intel(R)Core(TM) i7-14650HX	1
Memory	Samsung 16G DDR5	2
Graphics	GeForce RTX 4060	1
Hard disk	Western Digital 1TB	1

The hyperparameter settings for the experiment are shown in Table 2. The Image Size affects both the training accuracy and speed. The Batch Size determines the number of training samples used in each model update. Epoch refers to the number of complete passes through the training dataset. The Optimizer controls how the model's parameters are updated. The Number of Workers represents the number of parallel processes used for data loading during training. The Learning Rate determines the speed at which the network updates its weights during training. Patience is used to control early stopping or learning rate adjustment when the model's performance does not improve within the set number of epochs.

Table 2. Hyperparameter settings.

Name	Value
Image Size	640
Batch Size	16
Epochs	100
Optimizer	SGD
Number of Workers	8
Learning Rate	0.01
Patience	50

A total of 2615 images were used in the experiment, of which 2120 were collected by the research team using a drone while the rest were obtained from the Internet. The experiment included four types of defect detection, namely, tower, transmission line, insulator, and vibration hammer, and the detection categories are shown in Table 3.

Table 3. Overhead transmission line inspection categories.

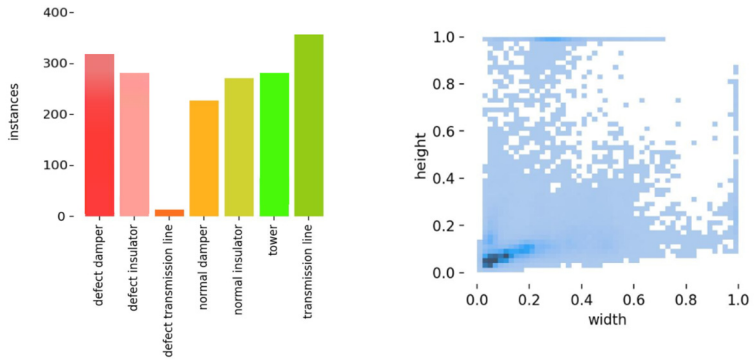
Testing Program	Defect Type
Insulator	Crack, broken
Damper	Corrosion, deformation
Tower	Corrosion, crack
Transmission line	Broken wire, disconnection

The transmission line picture dataset was labeled with data using Makesense.ai software; the defective areas were labeled and classified with data, the labeled rectangular box parameters were obtained, the text file was exported, and finally the dataset was sliced and divided into a training set, a validation set, and a test set in a ratio of 7:2:1. And it formatted so that it can be used for ABG-YOLOv8n model training. The result of the data labeling and slicing is shown in Figure 6, including images and rectangular box parameter labels.



Figure 6. Data labeling and slicing format.

After the dataset was made, pycharm was used to train the model, and the trained +weights file was used for model prediction. The distribution of sample labels is shown in Figure 7.



(**a**) (**b**)

Figure 7. (**a**) Distribution of label quantities in the dataset. (**b**) Distribution of label sizes.

The confusion matrix is a summary of the prediction results, presented in matrix form to display the classification accuracy. The horizontal axis represents the true class of the data, while the vertical axis represents the predicted class by the neural network. In this paper, the model's detection performance on the dataset is shown by plotting the confusion matrix, as illustrated in Figure 8. The background area is also treated as a category in the evaluation, reflecting the interference of complex environments in the detection of multiple types of defects.

From the confusion matrix, it can be seen that the improved model demonstrates a high classification accuracy in recognizing various defects, with a more balanced classification performance.

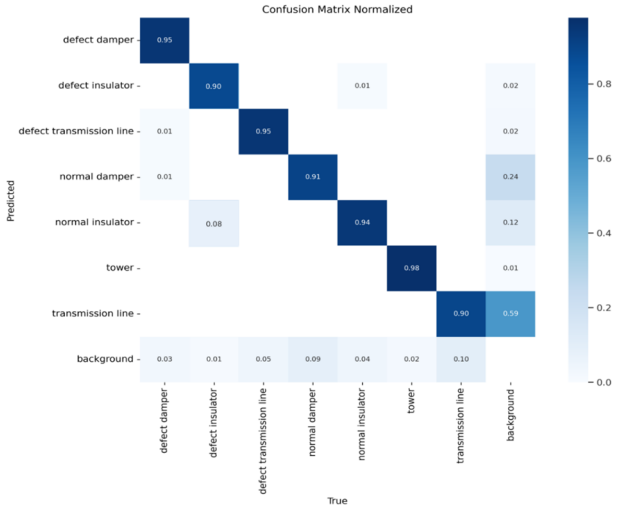


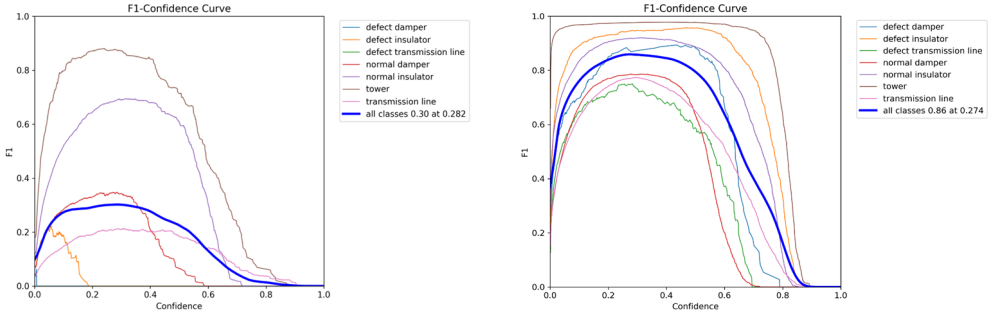
Figure 8. Confusion matrix.

3.2. Comparative Experiments

The YOLOv8n model was trained on the overhead transmission line dataset and deployed on the RV1126 edge computing device. The experimental results revealed that YOLOv8n performs poorly in detecting small and tiny objects and that the response time is too long due to limited computing resources in the edge device. To address these two key issues, the ABG-YOLOv8n model underwent a series of optimizations compared to the original YOLOv8n architecture.

(1) The lightweight GhostNetV2 module was used to solve the problem of prolonged response time when deploying the model on edge computing devices.
(2) SCConv replaced the standard convolutional layers to make the detection results more precise.
(3) The BiFPN scheme was employed to address the difficulty in detecting small objects, such as minor damage to dampers and insulators.
(4) The ASFF mechanism was introduced to further enhance the model's detection accuracy.

The performance comparison between the YOLOv8n model and the ABG-YOLOv8n model is shown in Figure 9. The figure displays the F1-Confidence curve, which evaluates the model's performance across different categories using the F1 score at various confidence thresholds.



(**a**) (**b**)

Figure 9. F1-Confidence curves of the YOLOv8n model (**a**) and the ABG-YOLOv8n model (**b**).

The experiment introduced other well-established models for comparison, as shown in Table 4. Faster R-CNN [23] performed worse in terms of precision and recall compared to the optimized YOLO models. The ABG-YOLOv8n model showed improvements in both precision and recall when compared to other improved YOLO models.

Table 4. Model parameter comparison.

Model	P/%	R/%	mAP@.5/%	mAP@0.5~0.95/%
Faster R-CNN [23]	88.7	87.1	79.6	40.1
Mask R-CNN	86.1	84.2	81.7	41.4
SSD	82.5	84.8	83.1	46.2
YOLOv8n	89.9	91.1	88.9	50.2
DCP-YOLOv8n [21]	92.1	93.4	90.1	52.2
ABG-YOLOv8n	93.5	93.1	93.4	52.8

The experiment introduced other lightweight backbone network modules for comparison, as shown in Table 5. GhostNetV2, while maintaining computational complexity, effectively improved the detection accuracy and efficiency, making the model suitable for deployment on devices with limited computational resources.

Table 5. Comparison of lightweight backbone network modules.

Module	mAP@.5/%	mAP@0.5~0.95/%	FLOPs/G
MobileNetV3	89.8	48.1	11.7
G_Ghost	90.8	42.8	12.1
GhostNetV2	90.6	48.4	10.1

The experiment introduced other networks that could enhance detection accuracy for comparison. As shown in Table 6, after integrating BiFPN and SCConv, YOLOv8n significantly improved the model's ability to detect small and fine-grained targets.

Based on the comparison experiment results, the ABG-YOLOv8n model effectively addressed the key issues through a series of optimizations. A comparison of the detection effects of the YOLOv8n model and the ABG-YOLOv8n model (b) is shown in Figure 10.

Table 6. Comparison of improved feature fusion network with other networks.

Module	P/%	R/%	mAP@.5/%	mAP@0.5~0.95/%
CCFM	91.7	89.4	87.1	83.5
Slim-Neck	90.6	90.1	86.7	83.0
HS-FPN	90.7	92.6	88.5	49.5
BiFPN	89.5	91.8	90.3	49.1
BiFPN + SDI	91.4	91.8	90.1	51.4
BiFPN + SCConv	92.7	92.1	92.5	51.2



(**a**) (**b**)

Figure 10. Comparison of the effects of the YOLOv8n model (**a**) and the ABG-YOLOv8n model (**b**).

3.3. Ablation Experiment

An ablation experiment was conducted with YOLOv8n as the baseline, gradually optimizing it, as shown in Table 7. The ABG-YOLOv8n model showed significant improvements across various parameters. Replacing the backbone network with GhostNetV2 led to a 3.3% increase in average precision and a 2.1% increase in mean precision. Additionally,

integrating BiFPN and SCConv into the feature fusion network and incorporating the ASFF mechanism in the detection head resulted in a 3.5% improvement in precision and a 2.2% increase in recall.

According to the experimental data, the fully configured ABG-YOLOv8n model demonstrated superior performance across all key metrics.

Table 7. Ablation experiment of ABG-YOLOv8n model.

GhostNetV2	BiFPN	SCConv	ASFF	P/%	R/%	mAP@.5/%	mAP@0.5~0.95/%
√			√	90.6	90.1	89.1	48.4
	√		√	91.5	91.8	91.3	49.1
	√	√	√	93.7	92.1	92.5	51.2
√	√	√	√	93.5	93.1	93.4	50.1

In the table, the "√" symbol indicates that the module is incorporated into the algorithm. It shows which model elements are included in the algorithm for each ablation experiment.

4. Conclusions

This paper presents a study on defect detection for overhead transmission lines based on the improved YOLOv8n model. To address the issues of YOLOv8n's poor detection performance for small and tiny objects and its prolonged response time when deployed on edge computing devices, due to limited computational resources, the ABG-YOLOv8n model introduces several key improvements:

GhostNetV2, a lightweight model from Huawei's mobile platform, was adopted to replace the feature extraction network of YOLOv8n, significantly reducing the network parameters and computational load while maintaining good feature representation capabilities. In the feature fusion layer, BiFPN was used to replace PANet in YOLOv8n, further improving the model's performance in multi-scale object detection and making detection results more precise. SCConv was employed instead of the standard convolution layers in YOLOv8n, enhancing feature representation by processing spatial and channel information simultaneously, improving detection accuracy and robustness, and more effectively capturing spatial relationships and channel features of objects. The detection head introduced the ASFF mechanism, which dynamically adjusts the weights of feature maps at different scales, thereby better combining features of various sizes during object detection, improving the model's sensitivity to targets of different sizes and detection accuracy. Finally, an experimental platform and simulation models were built for comparative experiments with several models.

After a series of experimental validations, the ABG-YOLOv8n model fully balances detection performance and detection efficiency. Although the problem of inaccurate detection of small targets may occur at long distances, this can be remedied by deploying the model on a UAV platform with the support of hardware devices.

The model can also be widely deployed in future detection application scenarios, relying on the lightweight design of the model, which can be deployed on resource-constrained edge computing devices such as Nvidia jetson and rknn. It can ensure both detection in real time and detection accuracy.

In summary, the ABG-YOLOv8n model proposed in this paper significantly outperforms the YOLOv8n model, which is of great significance for future vision applications on mobile and edge devices.

Author Contributions: Conceptualization, Y.Y.; Methodology, H.L.; Software, Y.Y.; Validation, Y.Y.; Investigation, W.C. and Y.W.; Data curation, Y.Y.; Writing—original draft, Y.Y.; Writing—review & editing, H.L. All authors have read and agreed to the published version of the manuscript.

Funding: This research received no external funding.

Data Availability Statement: The data presented in this study are available on request from the corresponding author. The data are not publicly available due to the data is jointly owned by other team members.

Conflicts of Interest: The authors declare no conflict of interest.

References

1. Fayazi, M.; Saffarian, A.; Joorabian, M.; Monadi, M. An AI-based fault detection and classification method for hybrid parallel HVAC/HVDC overhead transmission lines. *Electr. Power Syst. Res.* **2025**, *238*, 111083. [CrossRef]
2. Wang, S.; Li, Q.; Yang, T.; Li, Z.; Bai, D.; Tang, C.; Pu, H. LSD-YOLO: Enhanced YOLOv8n Algorithm for Efficient Detection of Lemon Surface Diseases. *Plants* **2024**, *13*, 2069. [CrossRef] [PubMed]
3. Salem, A.A.A.; Lau, Y.K.; Saida, A.A. Detection of overhead line glass insulator condition using dual function device and deep learning approach. *Comput. Electr. Eng.* **2024**, *120*, 109764. [CrossRef]
4. Zhang, Z.; Tan, L.; Robert, K.L.T. An Improved Fire and Smoke Detection Method Based on YOLOv8n for Smart Factories. *Sensors* **2024**, *24*, 4786. [CrossRef] [PubMed]
5. Zhao, L.; Zhang, Y.; Dou, Y.; Jiao, Y.; Liu, Q. ETLSH-YOLO: An Edge–Real-Time Transmission Line Safety Hazard Detection Method. *Symmetry* **2024**, *16*, 1378. [CrossRef]
6. Zhang, Z.; Tan, L.; Tiong, K.L.R. Ship-Fire Net: An Improved YOLOv8 Algorithm for Ship Fire Detection. *Sensors* **2024**, *24*, 727. [CrossRef]
7. Chen, T.; Dong, L.; She, X. Research on Automatic Counting of Drill Pipes for Underground Gas Drainage in Coal Mines Based on YOLOv7-GFCA Model. *Appl. Sci.* **2023**, *13*, 10240. [CrossRef]
8. Zheng, Z.; Chen, N.; Wu, J.; Xv, Z.; Liu, S.; Luo, Z. EW-YOLOv7: A Lightweight and Effective Detection Model for Small Defects in Electrowetting Display. *Processes* **2023**, *11*, 2037. [CrossRef]
9. Li, Z.; Fang, X.; Zhen, T.; Zhu, Y. Detection of Wheat Yellow Rust Disease Severity Based on Improved GhostNetV2. *Appl. Sci.* **2023**, *13*, 9987. [CrossRef]
10. Yang, Z.; Shao, Y.; Wei, Y.; Li, J. Precision-Boosted Forest Fire Target Detection via Enhanced YOLOv8 Model. *Appl. Sci.* **2024**, *14*, 2413. [CrossRef]
11. Li, X.; Zhou, H.; Zhao, M. Transformer-based cascade networks with spatial and channel reconstruction convolution for deepfake detection. *Math. Biosci. Eng. MBE* **2024**, *21*, 4142–4164. [CrossRef] [PubMed]
12. Mo, H.; Wei, L. Fine Segmentation of Chinese Character Strokes Based on Coordinate Awareness and Enhanced BiFPN. *Sensors* **2024**, *24*, 3480. [CrossRef] [PubMed]
13. dos Santos, P.R.S.; de Carvalho Brito, V.; de Carvalho Filho, A.O.; Diniz, J.O.B. KochDet: BiFPN-based deep architecture for tuberculosis diagnosis. *Biomed. Signal Process. Control.* **2024**, *91*, 91106056. [CrossRef]
14. Zheng, L.; Yi, J.; He, P.; Tie, J.; Zhang, Y.; Wu, W.; Long, L. Improvement of the YOLOv8 Model in the Optimization of the Weed Recognition Algorithm in Cotton Field. *Plants* **2024**, *13*, 1843. [CrossRef] [PubMed]
15. Kaihua, Z.; Haikuo, S. Solder Joint Defect Detection in the Connectors Using Improved Faster-RCNN Algorithm. *Appl. Sci.* **2021**, *11*, 576. [CrossRef]
16. Qun, L.; Zhendong, L. Research on Face Local Attribute Detection Method Based on Improved SSD Network Structure. *Adv. Multimed.* **2022**, *2022*, 3730529.
17. Zhou, X.; Zhang, L. SA-FPN: An effective feature pyramid network for crowded human detection. *Appl. Intell.* **2022**, *52*, 12556–12568. [CrossRef]
18. Xu, C.; Xin, M.; Wang, Y.; Gao, J. An efficient YOLO v3-based method for the detection of transmission line defects. *Front. Energy Res.* **2023**, *11*, 1236915. [CrossRef]
19. Liu, G.; Li, Z.; Sun, X.; Tian, Y.; Li, M. Transmission line image defect diagnosis based on YOLOv3 and SNIPER cascade lifting algorithm. *IOP Conf. Ser. Earth Environ. Sci.* **2019**, *332*, 042032. [CrossRef]
20. Chen, W.; Ding, Y.; Lin, M.; Song, H.; Li, T.; Gong, S. Research on Anti-breakage Target Detection Method of Transmission Line based on Improved YOLOv5. *J. Phys. Conf. Ser.* **2024**, *2774*, 012035. [CrossRef]
21. Wang, Y.; Zhang, L.; Xiong, X.; Kuang, J.; Xiang, S. A Lightweight and Efficient Multi-Type Defect Detection Method for Transmission Lines Based on DCP-YOLOv8. *Sensors* **2024**, *24*, 4491. [CrossRef] [PubMed]
22. Sun, H.; Shen, Q.; Ke, H.; Duan, Z.; Tang, X. Power Transmission Lines Foreign Object Intrusion Detection Method for Drone Aerial Images Based on Improved YOLOv8 Network. *Drones* **2024**, *8*, 346. [CrossRef]
23. Jia, W.; Jian, L.; Qi, R. Application of artificial intelligence image recognition technology based on Faster-R CNN in automatic inspection of power transmission and transformation. *J. Phys. Conf. Ser.* **2022**, *2306*, 012006.

Disclaimer/Publisher's Note: The statements, opinions and data contained in all publications are solely those of the individual author(s) and contributor(s) and not of MDPI and/or the editor(s). MDPI and/or the editor(s) disclaim responsibility for any injury to people or property resulting from any ideas, methods, instructions or products referred to in the content.